Theor Chem Acc (2011) 129:73–84
DOI 10.1007/s00214-011-0892-1

REGULAR ARTICLE

Hydrogen abstraction reactions of OH radicals with $CF_2ClCClXH$ (X = F, Cl) and $CFCl_2CClXH$ (X = F, Cl): a mechanistic and kinetic study

Li Wang · Yuan Zhao · Jinglai Zhang

Received: 9 September 2010 / Accepted: 11 January 2011 / Published online: 29 January 2011

Abstract The reactions of OH (OD) radicals with $CF_2ClCClFH$ (R1), CF_2ClCCl_2H (R2), $CFCl_2CClFH$ (R3), and $CFCl_2CCl_2H$ (R4) have been investigated theoretically by a dual-level direct dynamics method. The optimized geometries and frequencies of the stationary points are calculated at the MPW1K/6-311+G(d,p) level. To improve the reaction enthalpy and potential barrier of each reaction channel, the single-point energy calculation is made by the MC-QCISD method. The enthalpies of formation of the species $CF_2ClCClFH$, CF_2ClCCl_2H, $CFCl_2CClFH$, $CFCl_2CCl_2H$, $CF_2ClCClF$, CF_2ClCCl_2, $CFCl_2CClF$, and $CFCl_2CCl_2$ are evaluated by two sets of isodesmic reactions. Using canonical variational transition state theory (CVT) with the small-curvature tunneling correction (SCT) method, the rate constants of OH and OD radicals with $CF_2ClCClXH$ (X = F, Cl) and $CFCl_2CClXH$ (X = F, Cl) are evaluated over a wide temperature range of 100–2,000 K at the MC-QCISD//MPW1K/6-311+G(d,p) level. The calculated CVT/SCT rate constants are consistent with available experimental data. The results show that the tunneling correction has an important contribution in the calculation of rate constants at lower temperatures. For the above-mentioned four reactions, the kinetic isotope effects are also calculated. Finally, the effect of fluorine or chlorine substitution on reactivity of the C–H bond is discussed.

Keywords $CF_2ClCClXH$ (X = F, Cl) · $CFCl_2CClXH$ (X = F, Cl) · Rate constants · Direct dynamics method · Kinetic isotopic effect

1 Introduction

Chlorofluorocarbons (CFCs) contribute to two very important global ecological consequences with their emission into the atmosphere. One is that the photolysis of CFCs by ultraviolet solar radiation produces chlorine atoms that can initiate the chain destruction of ozone. The other is that CFCs contribute to global warming by absorbing the Earth's infrared emission [1–3]. Partly halogenated alkanes (HCFCs) are of interest as possible CFCs substitutes since they retain many desirable properties of CFCs and have less ozone depletion potential. Here, we focus our attention on four species, i.e., HCFC-122(CF_2ClCCl_2H), HCFC-121 ($CFCl_2CCl_2H$), HCFC-123a($CF_2ClCClFH$), and HCFC-122a ($CFCl_2CClFH$). Among them, CF_2ClCCl_2H and $CFCl_2CCl_2H$ are mainly used for refrigerants, foaming agents, fire extinguishing agent, and other applications. As to HCFC-123a ($CF_2ClCClFH$) and HCFC-122a ($CFCl_2CClFH$), they have not been applied in large scale of industrial applications although their structures are similar to CF_2ClCCl_2H and $CFCl_2CCl_2H$. However, their kinetic parameters have also been studied here for comparison with CF_2ClCCl_2H and $CFCl_2CCl_2H$. HCFCs can react with the tropospheric hydroxyl radicals and therefore have a smaller chance for reaching the stratosphere. These reactions are the main chemical removal processes that determine the

Electronic supplementary material The online version of this article (doi:10.1007/s00214-011-0892-1) contains supplementary material, which is available to authorized users.

L. Wang · Y. Zhao · J. Zhang (✉)
Institute of Environmental and Analytical Sciences,
College of Chemistry and Chemical Engineering,
Henan University, 475004 Kaifeng, Henan,
People's Republic of China
e-mail: zhangjinglai@henu.edu.cn

atmospheric lifetime for such substances in the troposphere. Thus, accurate data for the rate constants of above-mentioned four species with OH radicals and their temperature dependence are necessary and important [4].

Owing to their importance, a few experimental kinetic studies have been performed on the title reactions [5–8]. Orkin et al. [5] measured the rate constants of reaction $CF_2ClCClFH + OH \rightarrow CF_2ClCClF + H_2O$ (R1) in a temperature range from 298 to 460 K. Their results were fitted to a linear Arrhenius plot with a pre-exponential factor $A = (9.2^{+2.5}_{-2.0}) \times 10^{-13}$ cm^3 molecule^{-1}s^{-1} and an activation energy $E_a = 2.55 \pm 0.17$ kcal mol^{-1}. Two experiments were performed for the reaction of $CF_2ClCCl_2H + OH \rightarrow CF_2ClCCl_2 + H_2O$ (R2) and the rate-temperature expressions of (in cm^3 molecule^{-1}s^{-1}) $k_2 = (11.3^{+2.1}_{-1.6}) \times 10^{-13}\exp[-(918 \pm 52)/T]$ (298–460 K) and $k_2 = 8.3 \times 10^{-13}\exp[-893/T]$ (298–363 K) were obtained by Orkin et al. [5] and DeMore et al. [6], respectively. The results reported by Orkin et al. are higher than those obtained by DeMore et al., especially in the higher temperatures. Other two groups [7, 8] studied the reaction of $CFCl_2CClFH + OH \rightarrow CFCl_2CClF + H_2O$ (R3) in a temperature range of 294–460 K and got the corresponding Arrhenius expressions. It should be noted that the result measured by Orkin et al. [8] is unpublished. It was cited by Hsu et al. [7] in their paper for comparison. Up to now, no kinetic information is available for the reaction $CFCl_2CCl_2H + OH \rightarrow CFCl_2CCl_2 + H_2O$ (R4). Owing to the large number of possible isomeric compounds of HCFCs, laboratory measurement of every one is very time-consuming. It is therefore desirable to use theoretical method to study these reactions and extrapolate the rate constants to higher temperatures whenever possible.

Theoretically, Chiorboli et al. [9] used QSARs (quantitative structure–activity relationships) empirical model to estimate the rate constants of above-mentioned four reactions at room temperature. Unfortunately, they only obtained the rate constants at 298 K, and their results overestimated the experimental values with the maximum error of approximately four times. Thus, a detailed theoretical investigation is very desirable. Moreover, no kinetic or dynamic study has been performed for the isotopic substitution reactions of OD radicals with above-mentioned four species (denoted as R1′– R4′). The general purpose of this paper is to make a systematic theory survey on the dynamic properties of reactions of OH and OD radicals with four HCFCs' species. Specifically, we will focus on the importance of tunneling, the calculation of the Arrhenius parameters, and kinetic isotopic effect (KIE). Our results can be particularly useful for reactions R4 and R1′–R4′, for which no experimental rate constant has been measured.

For the molecule $CF_2ClCClFH$, 2C atom (see Fig. 1) is a chiral center, which has four different groups (H, F, Cl, and CF_2Cl) bonded to it. Thus, two chiral isomers of $CF_2ClCClFH$ should be found, i.e., R-$CF_2ClCClFH$ and S-$CF_2ClCClFH$. Since the energies of R- and S-$CF_2ClCClFH$ configurations are the same, the equivalent contribution of them to the rate constants can be assumed. So only the R-$CF_2ClCClFH$ isomer is considered in the present calculation. For the R-$CF_2ClCClFH$ configuration, three stable conformers are located, SC_{1a}, SC_{1b}, and SC_{1c}. Based on the calculation, the energies of them are on the order of $SC_{1a} < SC_{1b} < SC_{1c}$. SC_{1a} only is more stable than SC_{1b} and SC_{1c} by 0.4 and 0.5 kcal mol^{-1} at the MC-QCISD//MPW1K level, respectively, so it is likely that these three conformers have similar stability and will contribute to the overall rate constants. These channels are defined as following:

$$CF_2ClCClFH\ (SC_{1a}) + OH \rightarrow CF_2ClCClF + H_2O \quad \text{(R1a)}$$

$$CF_2ClCClFH\ (SC_{1b}) + OH \rightarrow CF_2ClCClF + H_2O \quad \text{(R1b)}$$

$$CF_2ClCClFH\ (SC_{1c}) + OH \rightarrow CF_2ClCClF + H_2O \quad \text{(R1c)}$$

For brevity, we will not detail the optical isomers and conformers of molecule $CFCl_2CClFH$ that are similar to those of the $CF_2ClCClFH$. The corresponding reaction channels are denoted as R3a, R3b, and R3c, i.e.,

$$CFCl_2CClFH\ (SC_{3a}) + OH \rightarrow CFCl_2CClF + H_2O \quad \text{(R3a)}$$

$$CFCl_2CClFH\ (SC_{3b}) + OH \rightarrow CFCl_2CClF + H_2O \quad \text{(R3b)}$$

$$CFCl_2CClFH\ (SC_{3c}) + OH \rightarrow CFCl_2CClF + H_2O \quad \text{(R3c)}$$

Conversely, there is no chiral center in the molecule CF_2ClCCl_2H. Two stable conformers, SC_{2a} and SC_{2b}, are located. The energy difference between SC_{2a} and SC_{2b} is only 0.5 kcal mol^{-1} at the MC-QCISD//MPW1k level, so both contributions coming from two conformers should be taken into account, i.e.,

$$CF_2ClCCl_2H\ (SC_{2a}) + OH \rightarrow CF_2ClCCl_2 + H_2O \quad \text{(R2a)}$$

$$CF_2ClCCl_2H\ (SC_{2b}) + OH \rightarrow CF_2ClCCl_2 + H_2O \quad \text{(R2b)}$$

Likewise, the reaction channels for reaction R4 are shown as following:

$$CFCl_2CCl_2H\ (SC_{4a}) + OH \rightarrow CFCl_2CCl_2 + H_2O \quad \text{(R4a)}$$

$$CFCl_2CCl_2H\ (SC_{4b}) + OH \rightarrow CFCl_2CCl_2 + H_2O \quad \text{(R4b)}$$

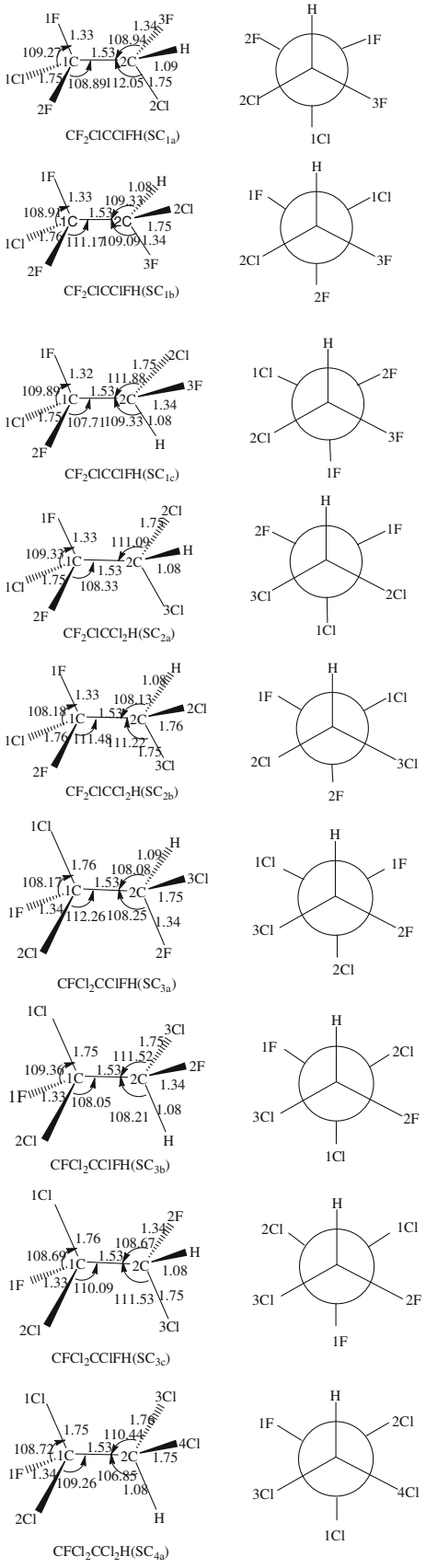

Fig. 1 Optimized geometries of reactants, OH radical, H_2O, and saddle points at the MPW1K/6-311+G(d,p) level. The values in the *parentheses* are experimental results [34]. Bond lengths are in *angstroms* and angles are in *degrees*

The dual-level direct dynamics method proposed by Truhlar et al. [10–14] is applied to investigate the dynamic properties of the title reactions. In this approach, the potential energy surface (PES) information is directly obtained from DFT (density functional theory) calculations and the rate constants are evaluated by the variational transition state theory (VTST) [15–17].

It is well known that the knowledge of the standard enthalpy of formation is important in determining the thermodynamic properties, the kinetics of atmospheric process, the stability of intermediate complexes, and the feasibility of reaction paths. However, there are no thermodynamic data available for all species included in these reactions except for species $CF_2ClCClFH$, OH radical, and H_2O. In the present study, we attempt to estimate the enthalpies of formation for these species via two sets of isodesmic reactions [18].

2 Calculation methods

All of the electronic structure calculations are made with the Gaussian 03 program [19]. The equilibrium geometries of all the stationary points, including the reactants, transition states (TSs), and products involved in the reactions, are calculated by modified Perdew–Wang 1-parameter model for kinetics (MPW1K) [20] with the 6-311+G(d,p) basis set (MPW1K/6-311+G(d,p)). The harmonic vibrational frequencies are calculated at the same level of theory to characterize the nature of each critical point and to make zero-point energy (ZPE) correction. The number of imaginary frequencies (0 or 1) indicates whether a minimum or a transition state has been located. To obtain more reliable reaction enthalpies and barrier heights, high-level single-point calculations for the stationary points are made at the multi-coefficient correlation method based on quadratic configuration interaction with single and double excitations (MC-QCISD) level [21]. In addition, the stationary geometries of reaction channel R1a are optimized using the BMK [22] and M06-2X [23] functionals with the 6-311+G(d,p) basis set. Various high-level single-point calculations are made for R1a by MCG3-DFT [24] (including MCG3-MPWPW91, MCG3-MPWB95, and MCG3-TPSSK CIS), MCQCISD-DFT [24] (including MCQCISD-MP WPW91, MCQCISD-MPWB95, and MCQCISD-TPSSK CIS), and MLSE-DFT [25] (including MLSE-MPW1B95 and MLSE-TPSS1 KCIS) methods. We tested various high-level single-point methods using the MPW1K/6-311+

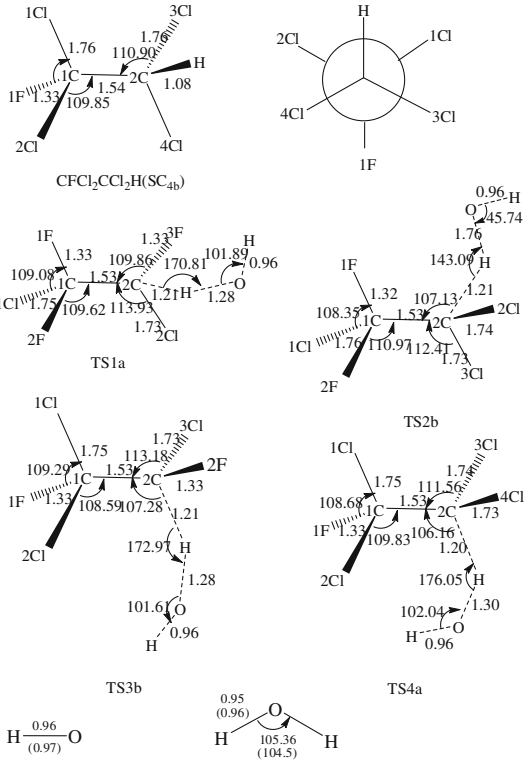

Fig. 1 continued

G(d,p), BMK/6-311+G(d,p), and M06-2X/6-311+G(d,p) geometries in order to find an affordable method for direct dynamics calculations that have high accuracy as judged by comparison with experimental activation energy.

Starting from the MPW1K saddle-point geometries and going downhill to both the asymptotic reactant and product channels, we construct the minimum-energy path (MEP) by the intrinsic reaction coordinate (IRC) theory. The IRC calculations are done with an even gradient step size of 0.05 $(\text{amu})^{1/2}$ bohr. Along this energy path, the reaction coordinate s is defined as the signed distance from the saddle point, with $s > 0$ referring to the product side. Also, first and second energy derivatives at geometries along the MEP are obtained to calculate the curvature of the reaction path and to calculate the generalized vibrational frequencies along the reaction path. The dual-level potential profile along the reaction path is further refined with the interpolated single-point energy (ISPE) method [26]. As pointed out in Chuang and Truhlar's paper [26], at least four points are very necessary to correct the low-level reaction path: two points very close to the saddle point that are used to locate the dual-level saddle point and two points close to the turning points for the tunneling calculation. Four non-stationary points (±0.05, around ±1.0) for the present system are used to correct the lower-level reaction path.

By means of the Polyrate 9.7 program [27], the rate constants for each reaction channel is calculated using the conventional transition state theory (TST) and canonical variational transition state theory (CVT) [28–30], and the tunneling correction is considered by the centrifugal-dominant small-curvature semiclassical adiabatic ground-state (CD-SCSAG) [31, 32] method, which is computed with equal segments in the Boltzmann and θ integrals, and the number of Gauss–Legendre quadrature points is chosen as 40 for computing the Boltzmann average. Also, the sixth-order Lagrangian interpolation is used to obtain the values of the effective mass for the CD-SCSAG tunneling calculation. In the present study, all vibrations are treated in the harmonic oscillator approximation for all reactions. Since the vibrational partition function is very sensitive to the low frequencies, we list the five lowest harmonic vibrational frequencies of the reactants and saddle points (the imaginary frequencies are also listed) in Table 1. As shown in Table 1, reactions R1–R4 have torsions in reactants and saddle points. But all of them are complicated motions involving more than one torsion or mixtures of torsion and bending. For example, mode 18 of the reactant $CF_2ClCClFH$ (SC_{1a}) in Table 1 is a complicated motion involving two torsions, that is, simultaneous torsions by the CF_2Cl group and the CClFH group. As mentioned by Truhlar et al. [33], the harmonic-oscillator approximation for this mode should be used, since no validated method is currently available to treat this kind of complicated torsion motion accurately. The two electronic states for OH radicals, with a 140 cm^{-1} splitting in the $^2\Pi$ ground state, are included in calculating its electronic partition functions. The curvature components are calculated by using a quadratic fit to obtain the derivative of the gradient with respect to the reaction coordinate.

To evaluate the heats of formation ($\Delta H^0_{f\,298}$) of the above-mentioned species, we made the calculations at the MC-QCISD//MPW1K/6-311+G(d,p) level using the following isodesmic reactions:

$$\begin{gathered}\text{For } CF_2ClCClFH\ (SC_{1a},\ SC_{1b},\ \text{or } SC_{1c}) \\ CF_2ClCClFH + CH_4 \rightarrow CH_3CH_2F + CF_2Cl_2\end{gathered} \quad \text{(R5)}$$

$$CF_2ClCClFH + C_2H_6 \rightarrow CH_3CF_2Cl + CH_3CClFH \quad \text{(R6)}$$

$$\begin{gathered}\text{For } CF_2ClCCl_2H\ (SC_{2a}\text{or } SC_{2b}) \\ CF_2ClCCl_2H + CH_4 \rightarrow CH_3CH_2F + CFCl_3\end{gathered} \quad \text{(R7)}$$

$$CF_2ClCCl_2H + C_2H_6 \rightarrow CH_3CF_2Cl + CH_3CCl_2H \quad \text{(R8)}$$

$$\begin{gathered}\text{For } CFCl_2CClFH\ (SC_{3a},\ SC_{3b}\ \text{or } SC_{3c}) \\ CFCl_2CClFH + CH_4 \rightarrow CH_3CH_2F + CFCl_3\end{gathered} \quad \text{(R9)}$$

$$CFCl_2CClFH + C_2H_6 \rightarrow CH_3CCl_3 + CH_2FCH_2F \quad \text{(R10)}$$

Table 1 The lowest five vibrational frequencies for the reactants and saddle points of R1–R4 (in cm^{-1}) calculated at the MPW1K/6-311+G(d,p) level

Mode	R1a	R1b	R1c	R2a	R2b	R3a	R3b	R3c	R4a	R4b
	SC_{1a}	SC_{1b}	SC_{1c}	SC_{2a}	SC_{2b}	SC_{3a}	SC_{3b}	SC_{3c}	SC_{4a}	SC_{4b}
18	80	79	78	72	80	89	83	77	69	81
17	177	174	172	174	175	173	171	168	174	174
16	207	247	235	220	189	191	202	232	223	181
15	324	274	322	257	266	276	260	257	240	248
14	351	360	343	320	332	323	305	326	289	276
	TS1a	TS1b	TS1c	TS2a	TS2b	TS3a	TS3b	TS3c	TS4a	TS4b
	1471i	1579i	1555i	1365i	1477i	1487i	1514i	1583i	1419i	1487i
23	60	60	58	67	67	61	61	63	70	67
22	72	85	73	86	94	77	92	82	98	96
21	113	109	102	101	102	114	119	108	107	101
20	142	139	132	136	137	137	147	134	140	142
19	181	177	172	178	178	173	176	170	178	177

For $CFCl_2CCl_2H$ (SC_{4a} or SC_{4b})

$$CFCl_2CCl_2H + CH_4 \rightarrow CH_3CH_2F + CCl_4 \quad \text{(R11)}$$

$$CFCl_2CCl_2H + C_2H_6 \rightarrow CH_3CH_2F + CH_2ClCCl_3 \quad \text{(R12)}$$

For $CF_2ClCClF$,

$$CF_2ClCClF + CH_4 \rightarrow CH_3CHF + CF_2Cl_2 \quad \text{(R13)}$$

$$CF_2ClCClF + C_2H_6 \rightarrow CH_2CF_2Cl + CH_3CClFH \quad \text{(R14)}$$

For CF_2ClCCl_2,

$$CF_2ClCCl_2 + CH_4 \rightarrow CH_3CHF + CFCl_3 \quad \text{(R15)}$$

$$CF_2ClCCl_2 + C_2H_6 \rightarrow CH_2CF_2Cl + CH_3CHCl_2 \quad \text{(R16)}$$

For $CFCl_2CClF$,

$$CFCl_2CClF + CH_4 \rightarrow CH_3CHF + CFCl_3 \quad \text{(R17)}$$

$$CFCl_2CClF + C_2H_6 \rightarrow CH_3CCl_3 + CH_2FCHF \quad \text{(R18)}$$

For $CFCl_2CCl_2$,

$$CFCl_2CCl_2 + CH_4 \rightarrow CH_3CHF + CCl_4 \quad \text{(R19)}$$

$$CFCl_2CCl_2 + C_2H_6 \rightarrow CH_2ClCCl_3 + CH_3CHF \quad \text{(R20)}$$

3 Results and discussion

3.1 Stationary points

The geometries of all the stationary points (reactants, products, and transition states) are optimized at the MPW1K/6-311+G(d,p) level. Owing to the similarity, only the reactants, H_2O, OH radical, and transition states TS1a, TS2b, TS3b, and TS4a as the representatives along with the available experimental values [34] are shown in Fig. 1. And the geometric parameters of other stationary points (including product radicals and other transition states) are displayed in Supporting Material (Figure S1). It can be seen that the theoretical geometric parameters of OH and H_2O are in solid agreement with the corresponding experimental values with maximum error of 1%. Due to the R- and S-$CF_2ClCClFH$ configurations possessing the same energy, only the conformers of R-$CF_2ClCClFH$ configuration are considered. Three stable conformers of R-$CF_2ClCClFH$, SC_{1a}, SC_{1b}, and SC_{1c}, are found. As shown in Fig. 1, SC_{1a}, H lies between 1F and 2F; SC_{1b}, H lies between 1F and 1Cl, and 3F lies between 1Cl and 2F; and SC_{1c}, H lies between 1F and 1Cl, and 3F lies between 1F and 2F. For the reactant CF_2ClCCl_2H, two stable conformers, SC_{2a} and SC_{2b}, are found. SC_{2a}, H lies between 1F and 2F, with C_s symmetry, and SC_{2b}, H lies between 1F and 1Cl, with C_1 symmetry. The conformers of $CFCl_2CClFH$ and $CFCl_2CCl_2H$ that are similarly to those of $CF_2ClCClFH$ and CF_2ClCCl_2H, respectively, will not be detailed. To make these conformers clearly to be seen, the Newman projections of them are also presented in Fig. 1. On the contrary, only one stable conformer for each product radical (i.e., $CF_2ClCClF$, CF_2ClCCl_2, $CFCl_2CClF$, and $CFCl_2CCl_2$) is located in the present study. The transition state TS1a resembles the reactants more than the products with a smaller elongation of the C–H bond for 11% compared with the C–H equilibrium bond length in isolated $CF_2ClCClFH$ and a significant elongation of the H–O bond for 35% with respect to the equilibrium bond length in H_2O molecule. The elongation of the forming bond (H–O bond) is greater than that of the breaking bond (C–H bond), indicating that the TS1a proceeds via "early" transition state. A similar conclusion can be drawn from other transition states.

Except for reactant $CF_2ClCClFH$, there are no available experimental enthalpies of formation (ΔH^0_{f298}) for other

Table 2 Calculated enthalpies of formation at the MC-QCISD//MPW1K/6-311+G(d,p) level along with available experimental results at 298 K (in kcal mol^{-1})

	Average value and deviation	Experiment
$CF_2ClCClFH(SC_{1a})$	−169.9 ± 4.6	−175.97[a], −171.26[b]
$CF_2ClCClFH(SC_{1b})$	−169.5 ± 4.6	
$CF_2ClCClFH(SC_{1c})$	−169.5 ± 4.6	
$CF_2ClCCl_2H(SC_{2a})$	−127.0 ± 4.3	
$CF_2ClCCl_2H(SC_{2b})$	−126.5 ± 4.3	
$CFCl_2CClFH(SC_{3a})$	−121.9 ± 3.0	
$CFCl_2CClFH(SC_{3b})$	−121.8 ± 3.0	
$CFCl_2CClFH(SC_{3c})$	−121.5 ± 3.0	
$CFCl_2CCl_2H(SC_{4a})$	−79.6 ± 3.0	
$CFCl_2CCl_2H(SC_{4b})$	−79.1 ± 3.0	
$CF_2ClCClF$	−123.5 ± 4.6	
CF_2ClCCl_2	−84.4 ± 4.3	
$CFCl_2CClF$	−74.0 ± 3.3	
$CFCl_2CCl_2$	−35.5 ± 4.6	

[a] From Ref. [39]

[b] From Ref. [40]

species involved in the title reactions. Thus, in the present study, their ΔH^0_{f298} values are estimated by using two sets of isodesmic reactions R5–R20. First, the reaction enthalpies of R5–R20 are calculated at the MC-QCISD//MPW1K/6-311+G(d,p) level. Secondly, these theoretical results are combined with the known enthalpies of formation [35–39] to estimate the required enthalpies of formation of target species at 298 K. (The heats of formation of the reference compounds are listed in Table S1.) The calculated results are presented in Table S2. The enthalpies of formation of all species estimated by two sets of isodesmic reactions are well consistent with each other. Table 2 presents the average values and available results in the literature [40, 41]. Note that the error limits are computed by adding the maximum uncertainties of ΔH^0_{f298} values of the reference compounds taken from the literature. The calculated $\Delta H^0_{f298}$of three conformers of R-$CF_2ClCClFH$ configuration, −169.9 ± 4.6 kcal mol^{-1} for SC_{1a}, −169.5 ± 4.6 kcal mol^{-1} for SC_{1b}, and −169.5 ± 4.6 kcal mol^{-1} for SC_{1c}, agree well with the results −175.97 and −171.26 kcal mol^{-1} reported by AIChE [40] (American Institute of Chemical Engineers) and Vatani et al. [41], respectively. Thus, it is reasonable to believe that the ΔH^0_{f298}values for other species predicted at the same level are reliable.

The reaction enthalpies (ΔH^0_{298}) of $CF_2ClCClFH$ + OH (R1), CF_2ClCCl_2H + OH (R2), $CFCl_2CClFH$ + OH (R3), and $CFCl_2CCl_2H$ + OH (R4) calculated at the MPW1K/6-311+G(d,p) and MC-QCISD//MPW1K/6-311+G(d,p) levels are summarized in Table 3. Since the reaction

Table 3 Enthalpies (in kcal mol^{-1}) at the MPW1K/6-311+G(d,p) and MC-QCISD//MPW1K/6-311+G(d,p) Levels

	MPW1K/6-311+G(d,p) ΔH^0_{298}	MC-QCISD//MPW1K/6-311+G(d,p) ΔH^0_{298}
$CF_2ClCClFH(SC_{1a})$ + OH	−16.5	−21.2
$CF_2ClCClFH(SC_{1b})$ + OH	−16.5	−21.7
$CF_2ClCClFH(SC_{1c})$ + OH	−16.8	−21.7
$CF_2ClCCl_2H(SC_{2a})$ + OH	−20.2	−25.1
$CF_2ClCCl_2H(SC_{2b})$ + OH	−20.5	−25.6
$CFCl_2CClFH(SC_{3a})$ + OH	−14.8	−19.7
$CFCl_2CClFH(SC_{3b})$ + OH	−14.7	−19.7
$CFCl_2CClFH(SC_{3c})$ + OH	−15.1	−20.1
$CFCl_2CCl_2H(SC_{4a})$ + OH	−18.0	−23.4
$CFCl_2CCl_2H(SC_{4b})$ + OH	−18.6	−23.9

energies of R1a, R1b, and R1c are very close (since the product radical of each reaction channel is the same, the difference just comes from the different conformers of reactant. Moreover, the difference of different conformers of reactant is small.), here we select R1a, which possesses the lowest barrier height among them to compare with other reactions. Similarly, the reaction channels R2b, R3b, and R4a are chosen as the representative of reactions R2, R3, and R4, respectively. At the higher level, the calculated enthalpy of R1a (−21.2 kcal mol^{-1}) is larger than that of R2b (−25.6 kcal mol^{-1}). According to the Evans and Polanyi suggestion [42], the barrier heights for the atom transfer reactions should decrease with the exothermicity increasing. Thus, the barrier height of R2 should be lower than that of R1. The similar result can be got between R3 and R4. Is this estimation consistent with the change of the barrier height?

Schematic potential energy surface of the title reactions with zero-point energy (ZPE) corrections is plotted in Fig. 2a–d. Note that the energy of respective conformer is set to zero as a reference. It is obviously seen from Fig. 2a, b, the barrier heights of reaction R1 (including three channels, 2.87 kcal mol^{-1} for R1a, 2.91 kcal mol^{-1} for R1b, and 3.02 kcal mol^{-1} for R1c) are higher by about 1 kcal mol^{-1} than those of reaction R2 (including two channels, 2.03 kcal mol^{-1} for R2a and 2.02 kcal mol^{-1} for R2b), i.e., ΔE(R1) > ΔE(R2). So the barrier height increases when one hydrogen atom of $CF_2ClCClH_2$ is substituted by a fluorine atom, than when substituted by a chlorine atom. Similarly, the barrier heights of reaction R3 are larger than the ones of reaction R4. This result is in line with the change in the dissociation energy (D^o_{298}) of C–H bond. The C–H bond dissociation energy of $CF_2ClCClFH$ (99.8 kcal mol^{-1}) is larger than that of CF_2ClCCl_2H (96.0 kcal mol^{-1}) at the MC-QCISD//MPW1K level. Note that the conformer with the lowest energy is used to calculate the C–H bond

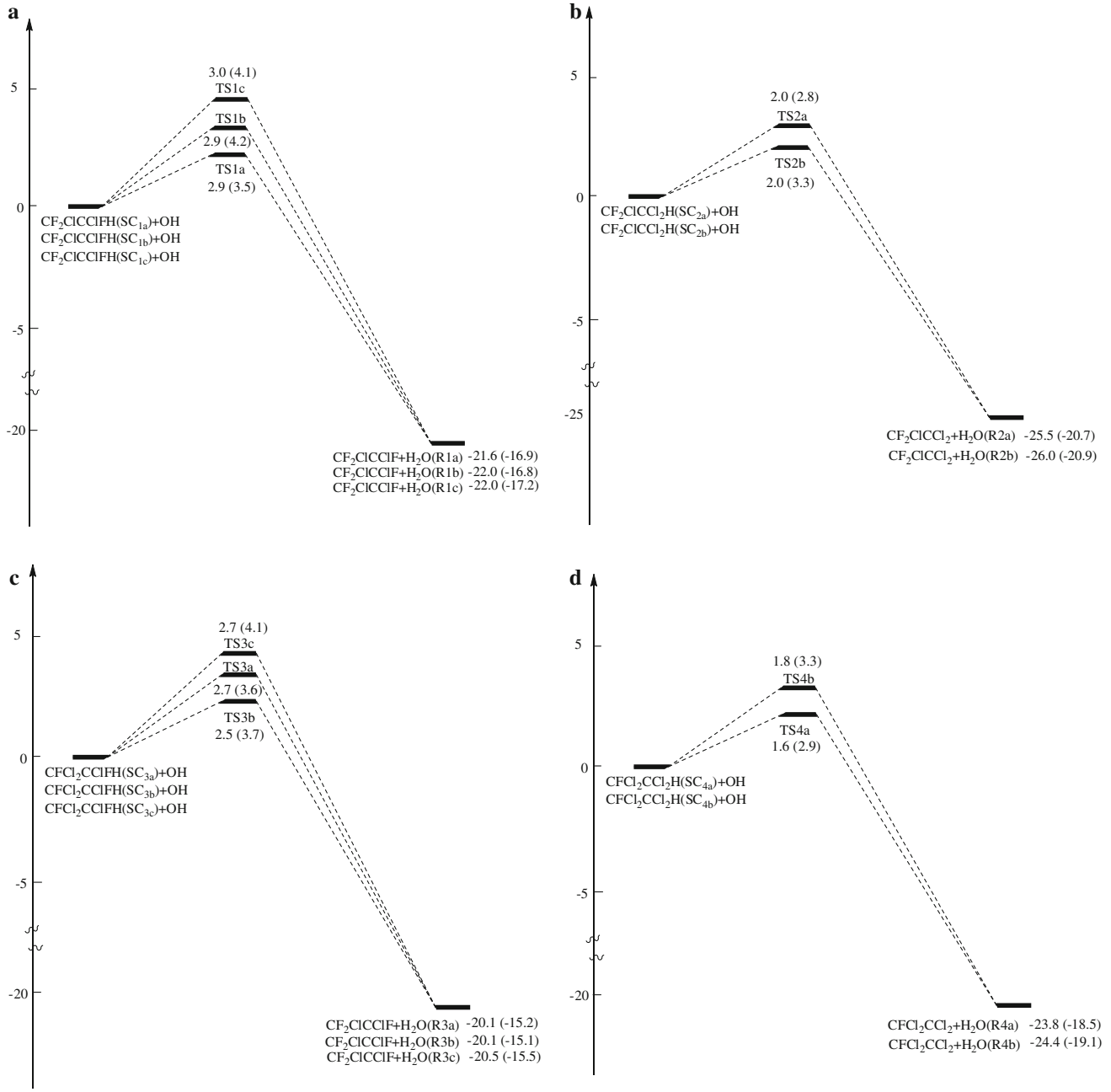

Fig. 2 **a** Schematic potential energy surface of the reaction $CF_2ClCClFH + OH$ (R1) with zero-point energy (ZPE) corrections at the MC-QCISD//MPW1K/6-311+G(d,p) level is in kcal mol^{-1}. The values in *parentheses* are those obtained at the MPW1K/6-311+G(d,p) level. **b** Schematic potential energy surface of the reaction $CF_2ClCCl_2H + OH$ (R2) with zero-point energy (ZPE) corrections at the MC-QCISD//MPW1K/6-311+G(d,p) level is in kcal mol^{-1}. The values in *parentheses* are those obtained at the MPW1K/6-311+G(d,p) level. **c** Schematic potential energy surface of the reaction $CFCl_2CClFH + OH$ (R3) with zero-point energy (ZPE) corrections at the MC-QCISD//MPW1K/6-311+G(d,p) level is in kcal mol^{-1}. The values in *parentheses* are those obtained at the MPW1K/6-311+G(d,p) level. **d** Schematic potential energy surface of the reaction $CFCl_2CCl_2H + OH$ (R4) with zero-point energy (ZPE) corrections at the MC-QCISD//MPW1K/6-311+G(d,p) level is in kcal mol^{-1}. The values in *parentheses* are those obtained at the MPW1K/6-311+G(d,p) level

dissociation energy. The value of $CFCl_2CClFH$ (101.4 kcal mol^{-1}) is larger than that of $CFCl_2CCl_2H$ by about 4 kcal mol^{-1} at the same level. However, the differences in C–H bond dissociation energy between $CF_2ClCClFH$ and $CFCl_2CClFH$ and between CF_2ClCCl_2H and $CFCl_2CCl_2H$ are not very large. Thus, the fluorine or chlorine substitution has almost no effect on the reactivity of H linking with the other carbon.

Table 4 Calculated barrier heights and activation energies (in kcal mol^{-1}) for R1a

Levels	ΔE	$E_{a,298}$
MC-QCISD//MPW1K/6-311+G(d,p)	2.9	1.5
MC-QCISD//BMK/6-311+G(d,p)	3.3	2.0
MC-QCISD//M06-2X/6-311+G(d,p)	3.3	2.1
MCG3-MPWPW91//MPW1K/6-311+G(d,p)	1.1	−0.4
MCG3-MPWPW91//BMK/6-311+G(d,p)	1.5	0.3
MCG3-MPWPW91//M06-2X/6-311+G(d,p)	1.7	0.4
MCG3-MPWB95//MPW1K/6-311+G(d,p)	0.9	−0.5
MCG3-MPWB95//BMK/6-311+G(d,p)	1.3	0.1
MCG3-MPWB95//M06-2X/6-311+G(d,p)	1.5	0.3
MCG3-TPSSKCIS//MPW1K/6-311+G(d,p)	1.0	−0.4
MCG3-TPSSKCIS//BMK/6-311+G(d,p)	1.4	0.2
MCG3-TPSSKCIS//M06-2X/6-311+G(d,p)	1.6	0.3
MCQCISD-MPWPW91//MPW1K/6-311+G(d,p)	1.1	−0.3
MCQCISD-MPWPW91//BMK/6-311+G(d,p)	1.6	0.3
MCQCISD-MPWPW91//M06-2X/6-311+G(d,p)	1.7	0.5
MCQCISD-MPWB95//MPW1K/6-311+G(d,p)	1.0	−0.5
MCQCISD-MPWB95//BMK/6-311+G(d,p)	1.4	0.1
MCQCISD-MPWB95//M06-2X/6-311+G(d,p)	1.6	0.3
MCQCISD-TPSSKCIS//MPW1K/6-311+G(d,p)	0.9	−0.6
MCQCISD-TPSSKCIS//BMK/6-311+G(d,p)	1.3	0.1
MCQCISD-TPSSKCIS//M06-2X/6-311+G(d,p)	1.5	0.2
MLSE-MPW1B95//MPW1K/6-311+G(d,p)	1.2	−0.2
MLSE-MPW1B95//BMK/6-311+G(d,p)	1.5	0.2
MLSE-MPW1B95//M06-2X/6-311+G(d,p)	1.7	0.4
MLSE-TPSS1 KCIS//MPW1K/6-311+G(d,p)	1.4	−0.01
MLSE-TPSS1KCIS//BMK/6-311+G(d,p)	1.7	0.4
MLSE-TPSS1KCIS//M06-2X/6-311+G(d,p)	1.9	0.7

In addition, the barrier height of reaction channel R1a is refined by nine multi-coefficient composite methods using the MPW1K/6-311+G(d,p), BMK/6-311+G(d,p), and M06-2X/6-311+G(d,p) geometries, respectively. The corresponding results are listed in Table 4. As can be seen from Table 4, the barrier heights refined by the same composite method on the geometries optimized by different density functionals are well consistent with the maximum error within 0.6 kcal mol^{-1}. So the geometries optimized by the MPW1K functional are reliable in the present study. Let us turn our attention to find which multi-coefficient composite method is suitable for reaction channel R1a. Among the tested various methods, MC-QCISD method predicts slightly higher barrier height than others. If we use the formula $E_{a,298} = \Delta E^* + nRT = V^* + \Delta ZPE + \Delta E(T) + nRT$ as a simple estimation of the activation energy [43], where V^*, ΔZPE, R, T, and $\Delta E(T)$ represent the potential barrier height, zero-point energy correction, gas constant, temperature, and thermal energy correction, the estimated activation energies at the MC-QCISD level are closest to the experimental value of 2.55 ± 0.17 kcal mol^{-1} for R1 [5] (Since channel R1a possesses the lowest barrier height among three channels of reaction R1, the disparity will become smaller after considering other two channels with higher barrier heights.), which indicates that the MC-QCISD method is a good choice to refine the energies for these systems. Thus, in the present study, we employ the MC-QCISD//MPW1K method to refine the potential energy surface and to calculate the rate constants.

3.2 Dynamics calculations

Dual-level (X//Y) direct dynamics calculations are made for these reactions by using the variational transition state theory with interpolated single-point energy (VTST-ISPE) approach. The rate constants for each reaction are evaluated by using the conventional transition state theory (TST), canonical variational transition state theory (CVT), and CVT with the small-curvature tunneling correction (SCT).

The TST, CVT, and CVT/SCT rate constants of reaction R1a are presented in Fig. 3. As can be seen from Fig. 3, the TST and CVT rate constants are nearly the same over a whole temperature range, which indicates that the variational effect on the rate constants is very small or almost negligible. However, the CVT/SCT rate constants are quite larger than those of TST and CVT at lower temperatures. The ratios of $k_{CVT/SCT}/k_{CVT}$ are 1,084 at 150 K, 104 at 200 K, 2.7 at 500 K, and 1.0 at 1,000 K for reaction R1a. Thus, small-curvature tunneling (SCT) correction plays an important role for reaction R1a at lower temperatures. The similar conclusion can be got from other reaction channels.

The CVT/SCT rate constants of k_{1a}, k_{1b}, k_{1c} and the total rate constants $k_1 = \omega_{1a}k_{1a} + \omega_{1b}k_{1b} + \omega_{1c}k_{1c}$ along with the available experimental values [5] are shown in Fig. 4a, where ω_{1a}, $\omega_{1b,}$ and ω_{1c} are the weight factors of each conformer calculated from the Boltzmann distribution function. Our calculated CVT/SCT rate constants agree well with the experimental results [5] in a temperature range of 298–460 K. Two experiments [5, 6] were performed for the reaction of $CF_2ClCCl_2H + OH \rightarrow CF_2ClCCl_2 + H_2O$ (R2). The calculated results $k_2 = \omega_{2a}k_{2a} + \omega_{2b}k_{2b}$, which are listed in Fig. 4b, are in reasonable agreement with both experimental ones except for the values at 370 K and 460 K reported by Orkin et al. [5] These two experimental values are obviously higher than other values. As shown from Fig. 4c, where the rate constants of reaction R3 ($k_3 = \omega_{3a}k_{3a} + \omega_{3b}k_{3b} + \omega_{3c}k_{3c}$) are plotted, the calculated rate constants of reaction R3 agree well with two sets of experimental results. The ratios of k(CVT/SCT)/k(experiment.) remain within a factor of 0.8 to 1.2 from 294 to 362 K. Moreover, the activation

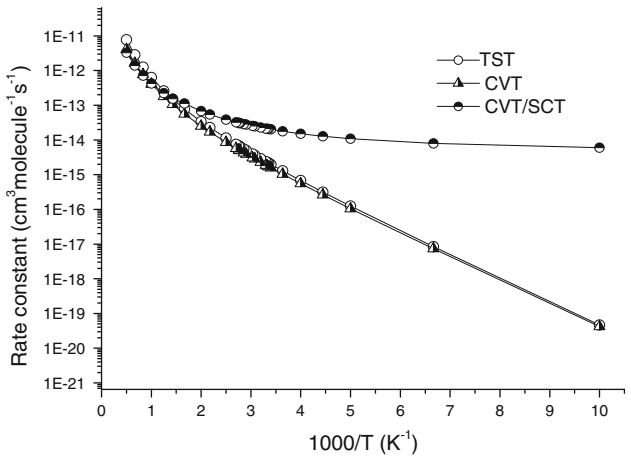

Fig. 3 Plot of the TST, CVT, and CVT/SCT rate constants calculated at the MC-QCISD//MPW1K/6-311+G(d,p) level versus 1,000/T between 100 and 2,000 K for the $CF_2ClCClFH(SC_{1a}) + OH \rightarrow CF_2ClCClF + H_2O$ (R1a)

energies of 1.2 kcal mol^{-1} (294–362 K) and 1.4 kcal mol^{-1} (298–460 K) agree well with the corresponding experimental ones of 2.3 and 2.5 kcal mol^{-1}, respectively [7, 8]. Furthermore, the present results calculated by dual-level direct dynamics method match better with the experimental ones than the values estimated by QSARs method [9]. Since the calculated rate constants of above three reactions produce well with the available experimental values, it is reasonable to infer that the rate constants of reaction R4 calculated at the same level are reliable, which are shown in Fig. 4d.

Another point concerns the kinetic isotope effect (KIE). The studies of the OH/OD kinetic isotope effect (KIE), which is defined as the ratio of OH and OD reactions rate constant, are shown in Table 5. The corresponding rate constants of OD radicals with above-mentioned four species, i.e., R1′– R4′, are shown in Fig. 5. By definition, a KIE is normal if it is greater than unity when the rate

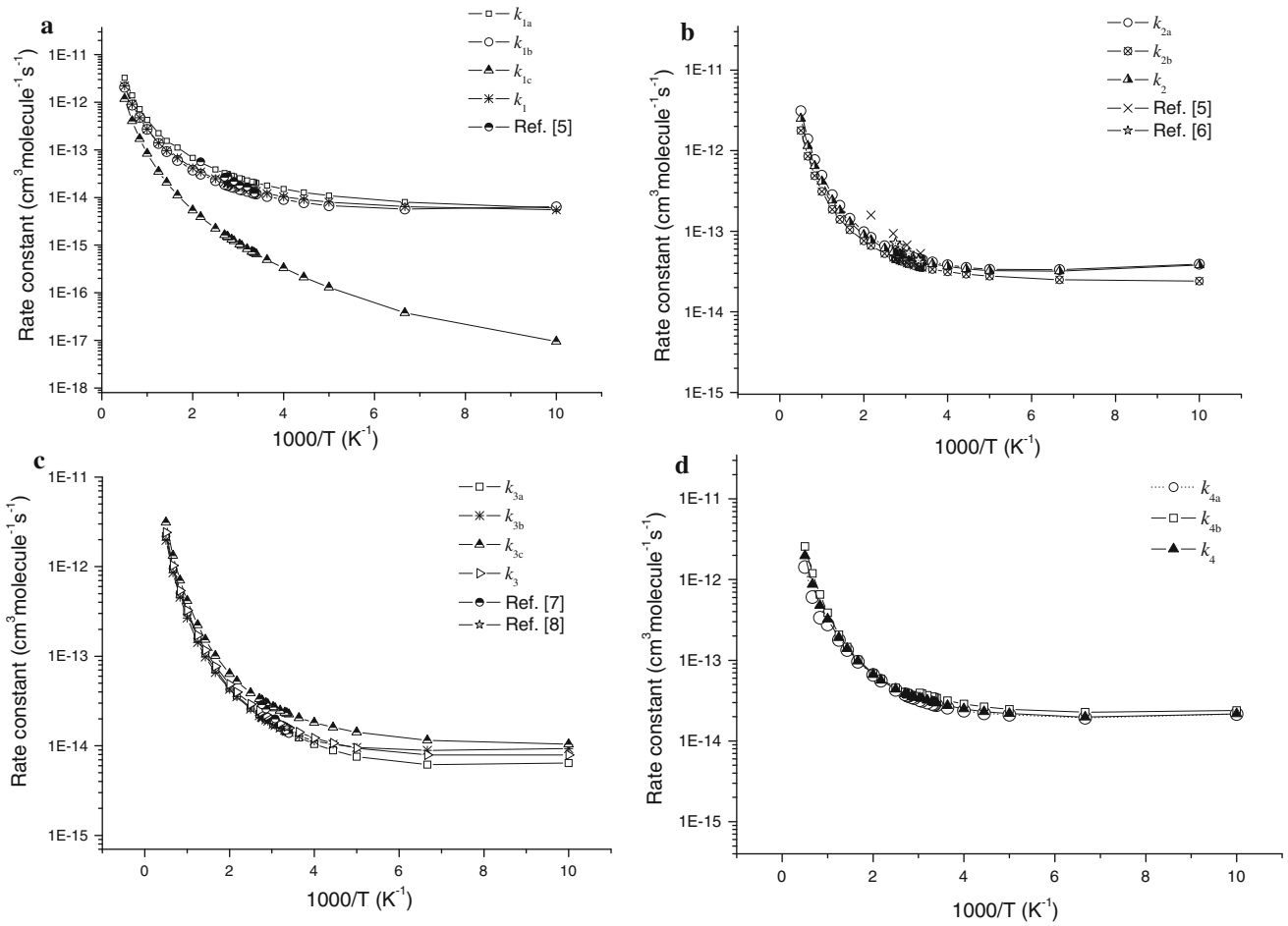

Fig. 4 **a** Plot of the calculated individual rate constants k_{1a}, k_{1b}, k_{1c}, the total rate constants k_1, and the available experimental values versus 1,000/T between 100 and 2,000 K. **b** Plot of the calculated individual rate constants k_{2a}, k_{2b}, the total rate constants k_2, and the available experimental values versus 1,000/T between 100 and 2,000 K. **c** Plot of the calculated individual rate constants k_{3a}, k_{3b}, k_{3c}, the total rate constants k_3, and the available experimental values versus 1,000/T between 100 and 2,000 K. **d** Plot of the calculated individual rate constants k_{4a}, k_{4b}, the total rate constants k_4, and the available experimental values versus 1,000/T between 100 and 2,000 K

Table 5 The ratios of k_H/k_D in a temperature range of 100–2,000 K

T(K)	k_1/k_1'	k_2/k_2'	k_3/k_3'	k_4/k_4'
100	0.4	1.5	1.2	1.2
200	0.6	1.0	1.2	1.1
298	0.8	1.0	1.1	1.1
300	0.8	1.0	1.1	1.1
400	0.9	1.0	1.1	1.1
500	0.9	1.0	1.1	1.1
600	1.0	1.0	1.1	1.1
700	1.0	1.0	1.1	1.1
800	1.0	0.9	1.1	1.1
1,000	1.0	0.9	1.1	1.1
1,200	1.0	1.0	1.1	1.1
1,500	1.0	1.0	1.0	1.1
2,000	1.0	1.0	1.0	1.0

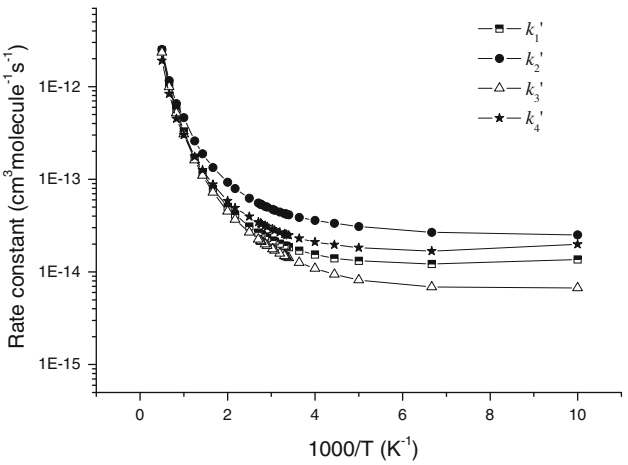

Fig. 5 Plot of the CVT/SCT rate constants calculated at the MC-QCISD//MPW1K/6-311+G(d,p) level versus 1,000/T between 100 and 2,000 K for the reactions R1′–R4′

constant for the lighter isotope is in the numerator, and it is an inverse isotope effect if it is less than unity. Reaction R1 exhibits inverse kinetic isotope effect at lower temperatures, whereas KIE increases with the increasing temperature. Conversely, other three reactions have slight and almost negligible inverse KIEs. Up to now, no experimental rate constant for reactions R1′–R4′ is available. Thus, to check the present deduction concerning the rate constants and KIEs, a deeper experimental study will be advisable.

We hope our calculated results will provide a good estimate for the kinetics of the reactions in other temperature range, which will be useful for the atmospheric modeling calculations and help to assess their atmospheric lifetimes of HCFCs. For convenience of further experimental measurements, the three-parameter expressions fitted for CVT/SCT rate constants for the reactions within

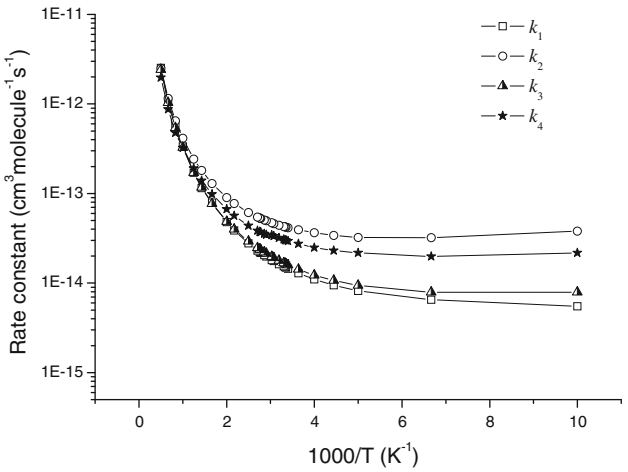

Fig. 6 Plot of the CVT/SCT rate constants calculated at the MC-QCISD//MPW1K/6-311+G(d,p) level versus 1,000/T between 100 and 2,000 K for the reactions R1–R4

Table 6 Arrhenius parameters for the title reactions

	A ($cm^3\ s^{-1}$)	E_a (kcal mol^{-1})
$CF_2ClCClFH + OH$ (R1)	1.1×10^{-13}	1.1
$CF_2ClCCl_2H + OH$ (R2)	1.3×10^{-13}	0.6
$CFCl_2CClFH + OH$ (R3)	1.1×10^{-13}	1.1
$CFCl_2CCl_2H + OH$ (R4)	1.0×10^{-13}	0.7

In a temperature range of 200–500 K

100–2,000 K are given as follows (in $cm^3molecule^{-1}s^{-1}$): $k_1 = 2.38 \times 10^{-23}T^{3.32}\exp(404.2/T)$, $k_2 = 9.53 \times 10^{-22}T^{2.81}\exp(467.9/T)$, $k_3 = 2.67 \times 10^{-23}T^{3.29}\exp(439.3/T)$, and $k_4 = 7.14 \times 10^{-22}T^{2.82}\exp(436.3/T)$.

3.3 Reactivity trends

The effect of fluorine or chlorine substitution on the reactivity of the C–H bond is evaluated by comparing CVT/SCT results that are plotted in Fig. 6. The pre-exponential factors (A) and activation energies (E_a) are fitted based on the calculated CVT/SCT rate constants in a temperature range of 200–500 K, which are summarized in Table 6. The CVT/SCT rate constants of R2 are about 2–4 times larger than those of R1 in a temperature range of 200–500 K. The calculated activation energy of R2 (0.6 kcal mol^{-1}) is almost half of that of R1 (1.1 kcal mol^{-1}), whereas the pre-exponential factors (A) are very close (1.3×10^{-13} vs. 1.1×10^{-13} $cm^3\ s^{-1}$) to each other. Thus, the increase in k mainly stems from the corresponding decrease in activation energy. The same conclusion can be got when comparison is made between R3 and R4. Our calculation indicates that C–H bond activity decreases when one hydrogen atom of $CF_nCl_{3-n}CClH_2$ ($n = 1, 2$) is substituted by a fluorine atom, than when substituted by a chlorine atom. It is easily seen that both pre-exponential factor (A) and

activation energy (E_a) do almost not change when comparison is made between R1 and R3. Thus, the rate constants of R1 and R3 are almost equal. The rate constants of R2 and R4 display the similar conclusion. Thus, the fluorine or chlorine substitution has almost no effect on the reactivity of H atom linking on the other carbon.

This conclusion is in line with the results obtained from the similar reactions that have been previously studied. Lots of experimental and theoretical studies have been performed for the hydrogen abstraction reactions of CF_3CClFH and CF_3CCl_2H with OH radicals [44, 45], Cl atoms [46–49], and F atoms [50–52]; among them, CF_3CCl_2H are the structural isomer of $CF_2ClCFClH$. All the results show that the rate constants increase with the increase in chlorine substitution. Conversely, no kinetic information is available for the reactions of CCl_3CF_2H and CCl_3CFClH, which are the structural isomers of CF_2ClCCl_2H and $CFCl_2CCl_2H$, respectively. Thus, the question arises: will the reactivity of C–H bond increase or decrease with the increase of chlorine substitution? It needs further studies to clarify this question.

4 Conclusion

In this paper, the hydrogen abstraction reactions of $CF_2ClCClXH$ (X = F, Cl) and $CFCl_2CClXH$ (X = F, Cl) with OH radicals are studied by dual-level direct dynamics method, along with four reactions of them with OD radicals. Dynamics calculations are made by using the variational transition state theory with interpolated single-point energies method (VTST-ISPE) at the MC-QCISD//MPW1K/6-311+G(d,p) level. For all the reactions, the variational effect is small and negligible at the whole measured temperatures, while the small-curvature tunneling effect plays an important role in a lower temperature range. We have provided reasonable theoretical values for the rate constants, which are especially useful in the case of the reaction R4 for which there are no well-determined experimental rate constants, along with the corresponding kinetic isotope effects. Our present study indicates that the fluorine atom substitution for one hydrogen atom of $CF_nCl_{3-n}CClH_2$ ($n = 1, 2$) leads to a decrease in the C–H bond reactivity when compared with the chlorine substitution.

On the other hand, the values of enthalpies of formation for $CF_2ClCClFH$, CF_2ClCCl_2H, $CFCl_2CClFH$, $CFCl_2CCl_2H$, $CF_2ClCClF$, CF_2ClCCl_2, $CFCl_2CClF$, and $CFCl_2CCl_2$ are calculated at the MC-QCISD//MPW1K/6-311+G(d,p) level by two sets of isodesmic reactions. Finally, the three-parameter expressions (in cm^3 $molecule^{-1}s^{-1}$) within 100–2,000 K are given: $k_1 = 2.38 \times 10^{-23}T^{3.32}\exp(404.2/T)$, $k_2 = 9.53 \times 10^{-22}T^{2.81}\exp(467.9/T)$, $k_3 = 2.67 \times 10^{-23}T^{3.29}\exp(439.3/T)$, and $k_4 = 7.14 \times 10^{-22}T^{2.82}\exp(436.3/T)$.

Acknowledgments We thank Professor Donald G. Truhlar for providing the POLYRATE 9.7 program. This work was supported by the National Natural Science Foundation of China (21003036), Science Foundation of Henan Province (2008A150005), Science Foundation of Henan University (2009YBZR013, SBGJ090507), Doctor Foundation of Henan University.

References

1. Talhaoui A, Louis F, Devolder P, Meriaux B, Sawerysyn JP (1996) J Phys Chem 100:13531
2. Liu R, Huie RE, Kurylo MJ (1990) J Phys Chem 94:3247
3. Rowland FS (1991) Annu Rev Phys Chem 42:731
4. Prather M, Spivakovsky CM (1990) J Geophys Res 95:18723
5. Orkin VL, Khamaganov VG (1993) J Atmos Chem 16:157
6. DeMore WB (1996) J Phys Chem 100:5813
7. Hsu KJ, DeMore WB (1995) J Phys Chem 99:1235
8. Orkin VL (1995) Personal communication
9. Chiorboli C, Piazza R, Tosato ML, Carassiti V (1993) Coord Chem Rev 125:241
10. Truhlar DG (1995) In: Heidrich D (ed) The reaction path in chemistry: current approaches and perspectives. Kluwer, Dordrecht, p 229
11. Truhlar DG, Garrent BC, Klippenstein SJ (1996) J Phys Chem 100:12771
12. Hu WP, Truhlar DG (1996) J Am Chem Soc 118:860
13. Hu WP, Liu YP, Truhlar DG (1994) J Chem Soc Faradav Trans 90:1715
14. Corchado JC, Coitiño EL, Chang YY, Fast PL, Truhlar DG (1998) J Phys Chem A 102:2424
15. Truhlar DG, Garrett BC (1980) Acc Chem Res 13:440
16. Truhlar DG, Isaacson AD, Garrett BC (1985) In: Baer M (ed) The theory of chemical reaction dynamics. CRC Press, Boca Raton, p 65
17. Truhlar DG, Garrett BC (1984) Annu Rev Phys Chem 35:159
18. IUPAC. http://www.iupac.org/reports/1999/7110minkin/i.html
19. Frisch MJ, Truck GW, Schlegel HB, Scuseria GE, Robb MA, Cheeseman JR, Zakrzewski VG, Montgomery JA, Stratmann RE Jr, Burant JC, Dapprich S, Millam JM, Daniels AD, Kudin KN, Strain MC, Farkas O, Tomasi J, Barone V, Cossi M, Cammi R, Mennucci B, Pomelli C, Adamo C, Clifford S, Ochterski J, Petersson GA, Ayala PY, Cui Q, Morokuma K, Malick DK, Rabuck AD, Raghavachari K, Foresman JB, Cioslowski J, Ortiz JV, Boboul AG, Stefnov BB, Liu G, Liaschenko A, Piskorz P, Komaromi L, Gomperts R, Martin RL, Fox DJ, Keith T, Al-Laham MA, Peng CY, Nanayakkara A, Gonzalez C, Challacombe M, Gill PMW, Johnson B, Chen W, Wong MW, Andres JL, Gonzalez C, Head-Gordon M, Replogle ES, Pople JA (2003) GAUSSIAN 03, Revision A.1, Guassian Inc., Pittsburgh
20. Lynch BJ, Truhlar DG (2001) J Phys Chem A 105:2936
21. Fast PL, Truhlar DG (2000) J Phys Chem 104:6111
22. Boese AD, Martin JML (2004) J Chem Phys 121:3405
23. Zhao Y, Truhlar DG (2008) Theor Chem Acc 120:215
24. Zhao Y, Lynch BJ, Truhlar DG (2005) Phys Chem Chem Phys 7:43
25. Sun YL, Li TH, Chen JL, Wu KJ, Hu WP (2007) Chem Phys Lett 442:220
26. Chuang YY, Corchado JC, Truhlar DG (1999) J Phys Chem 103:1140
27. Corchado JC, Chuang YY, Past PL, Hu WP, Liu YP, Lynch GC, Nguyen KA, Jackels CF, Fernandez-Ramos A, Ellingson BA, Lynch BJ, Zheng JJ, Melissas VS, Villa J, Rossi I, Coitino EL, Pu JZ, Albu TV, Steckler R, Garrett BC, Isaacson AD, Truhlar DG

(2007) POLYRATE, version 9.7. University of Minnesota, Minneapolis
28. Garrett BC, Truhlar DG (1979) J Chem Phys 70:1593
29. Garrett BC, Truhlar DG (1979) J Am Chem Soc 101:4534
30. Garrett BC, Truhlar DG, Grev RS, Magnuson AW (1980) J Phys Chem 84:1730
31. Lu DH, Truong TN, Melissas VS, Lynch GC, Liu YP, Garrett BC, Steckler R, Issacson AD, Rai SN, Hancock GC, Lauderdale JG, Joseph T, Truhlar DG (1992) Comput Phys Commun 71:235
32. Liu Y-P, Lynch GC, Truong TN, Lu D-H, Truhlar DG, Garrett BC (1993) J Am Chem Soc 115:2408
33. Zheng JJ, Truhlar DG (2010) Phys Chem Chem Phys 12:7782
34. Lide DR (1999) CRC handbook of chemistry and physics, 80th edn. CRC Press, New York
35. DeMore WB, Sander SP, Golden SP, Howard CJ, Golden DM, Kolb CE, Hampson RF, Molina MJ (1997) Chemical kinetics and photochemical data for use in stratospheric modeling, JPL Publication 97-4
36. Kolesov VP, Papina TS (1973) Russ J Phys Chem (Engl Transl) 47:1660
37. Lacher JR, Amador A, Park JD (1967) Trans Faraday Soc 63:1608
38. Manion JA (2002) J Phys Chem Ref Data 123
39. Zachariah MR, Westmoreland PR, Burgess DR Jr, Tsang W, Melius CF (1996) J Phys Chem 100:8737
40. Design Institute for Physical Properties Research (DIPPR), American Institute of Chemical Engineers, Project 801 (2006)
41. Vatani A, Mehrpooya M, Gharagheizi F (2007) Int J Mol Sci 8:407
42. Evans MG, Polanyi M (1938) Trans Faraday Soc 34:11
43. Schaffer F, Verevkin SP, Rieger HJ, Beckhaus HD, Ruchart C (1997) Liebigs Ann Chem 1333
44. Yamada T, Fang TD, Taylor PH, Berry RJ (2000) J Phys Chem A 104:5013
45. Cohen N, Westberg KR (1991) J Phys Chem Ref Data 20:1211
46. Wallington TJ, Hurley MD (1992) Chem Phys Lett 89:437
47. Tuazon EC, Atkinson R, Corchnoy SB (1992) Int J Chem Kinet 24:639
48. Warren RF, Ravishankara AR (1993) Int J Chem Kinet 25:833
49. Li B, Liu JY, Li ZS, Wu JY, Sun CC (2004) J Chem Phys 120:6019
50. Wallington TJ, Hurley MD, Shi J, Maricq MM, Sehested J, Nielsen OJ, Ellermann T (1993) Int J Chem Kinet 25:651
51. Sehested J (1994) Int J Chem Kinet 26:1023
52. Wang L, Zhao Y, Wang ZQ, Ju CG, Feng YL, Zhang JL (2010) J Mol Struc: Theochem 959:101